SCA2003-32: EFFECT OF GLAUCONITE ON PETROPHYSICAL PROPERTIES AS REVEALED BY CORE ANALYSIS

Wibeke Hammervold Thomas, Jon Knut Ringen, Sten Ola Rasch, Statoil ASA

This paper was prepared for presentation at the International Symposium of the Society of Core Analysts held in Pau, France, 21-24 September 2003

Abstract

During early-phase formation evaluation of a small sandstone reservoir in the North Sea logs and conventional core data indicated good reservoir quality (porosity: 30% & permeability 150mD). Both initial log and core-derived estimates of water saturation were high. However, the log-derived estimates were consistently lower than those from Dean-Stark core measurements and had a large degree of uncertainty. A well test produced oil and no water. The disagreement between log and core estimated was initially blamed on invasion of the core by the (non-traced) water-based drilling mud system. A second well was drilled using a traced oil-based system with plugs taken offshore to obtain quality connate water saturation data from cores. The results reduced the uncertainties in water saturation significantly although values were still high.

A special core analysis program was designed to include an investigation of the cause of the high water saturations, including *ESEM*, core drying effects, core resistivity, core petrography and relative permeability. Petrological analysis revealed a high proportion of a porous clay mineral, glauconite. The glauconite was distributed as pellets with high internal, water-bearing porosity. These pellets were randomly distributed throughout the matrix and were shown to be strongly water wet. The core analysis program revealed that this particular mineral with its properties gives special petrophysical characteristics to its host formation including:

- high connate water saturation values above the transition zone
- high porosity compared to permeability
- little variation in porosity with varying permeability
- porosity dependent on the air humidity during drying
- no linear RI/S_w-relationship
- resistivity measurements showing an effect opposite of the so-called "clay-effect"
- low residual oil saturation after water flooding

These formation characteristics were responsible for the uncertainty in log estimates of water saturation. The core analysis had therefore significantly reduced the project uncertainty. However, this glauconite issue is relatively uncommon in the North Sea and as a result it was sometimes hard to convince other disciplines to accept the results.

Introduction

Early appraisal during marginal field development requires reliance upon limited wireline and core data. Disagreements between core and wireline derived water saturation estimates in seemingly familiar clastic sandstone formation have historically been put down to core handling and preservation. Recent development in core acquisition and handling techniques (low invasion coring and the use of tracers to quantify mud invasion into the core) have demonstrably reduced these errors to a minimum, however, historical prejudges still remain within the industry.

When determining reservoir connate water saturation directly from core, the main focus should be on minimizing and correcting for invasion of water from the mud. Coring with an oil-based mud will usually leave the water saturation undisturbed and S_w can be determined by Dean-Stark (*DS*) [1] extraction of samples from the centre of the core. With a water-based mud, a tracer such as Deuterium or Tritiated water must be used to be able to correct for invasion. With water-based mud, plug samples must be drilled from the centre of the core at well site to minimize redistribution of invaded water to the centre of the core[2]. For both mud types it is possible that in the case of high water saturations, mobile water can be expelled from the core upon retrieval from the well due to pressure reduction.

Southern North Sea Field Example

Statoil has appraised one such marginal field during the 1990's. The field comprises of approximately 40m thick, shallow marine sandstone reservoir. Reservoir quality varies relatively little for the main field with porosities 31-32% and permeabilities of 100-200mD.

The discovery well on the field acquired core from the entire reservoir section using a non-traced, water-based mud system. Both initial wireline and core-derived estimates of water saturation were high. However, whilst logs suggested values of 20-40%, the *DS* values were much higher; in the range of 60-65%, Figure 1. The *DS* values were considered unreliable due to possible invasion of a water-based mud. We had not been successful in applying tracers to the mud in the first well, partly due to objections from the local authorities. The well was tested producing only oil, seemingly confirming the lower range of S_w.

Under planning of the second well, water saturation was recognised as the major target for the data acquisition program. An oil-based mud system with an emulsified water-phase was used where the water-phase was traced to ensure full correction of any mud invasion. Centre-plugs were drilled offshore with refined oil for *DS* measurements to limit the time for any fluid redistribution and evaporation. A conventional core analysis program was performed when the core arrived the laboratory. The results from the new *DS* tests (both offshore plugs and conventional plugs) confirmed high water saturations between 40-50%. No corrections for mud-invasion were necessary, see Figure 2 A fuller picture was now beginning to emerge with the arrival of petrographic, *ESEM*, capillary pressure and

resistivity data from the discovery well which addressed the differences between log and core S_w estimates and are discussed in the following sections.

A third well was drilled, including a sidetrack, indicating even more extreme S_w values from *DS* of between 55-70%. Again, a test in this well flowed oil with no water-production.

Special Core Analysis Programme

Mineral Analysis, ESEM & Wettability

When the high S_w values from the *DS* tests from the discovery well were confirmed by the *DS* data from the second well, the importance of petrography was recognised. The formation was understood to be fine grained (Thin section 1), indicating the potential for capillary bound water, but traditional sources of clay-bound water were low (kaolinites & smectites). The clay mineral glauconite was detected early on in significant volumes (18-30%), however, its petrophysical properties were not fully appreciated.

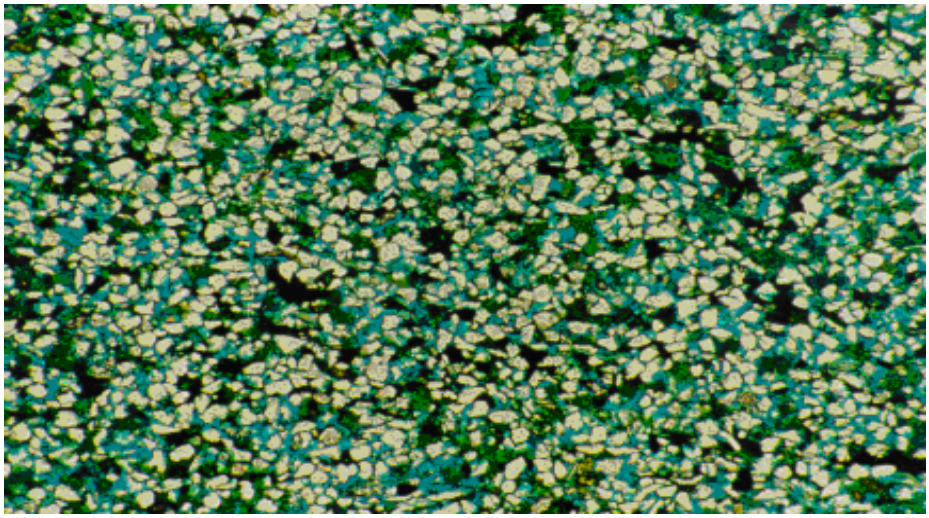

Thin section 1: Illustration of the fine-grained nature of the sands. Magnification x30.

The glauconite exists in two main forms: rounded pellets and glauconitised, altered mica flakes (Thin section 2). A third, rare, form consists of glauconite grain coatings. The internal porosity in the glauconite has been estimated at ~40%. An Environmental Scanning Electron Micro-scope (*ESEM*) was used to determine if this micro-intra-granular porosity in the glauconite contained oil or water. The *ESEM* technique[3] makes it possible to operate with fresh, unclean samples at near room conditions. 3 important tests and observations were made:

1) The glauconite was associated with high chloride values rather than carbon or sulphur indicating associated water rather than oil.

2) Sample vacuuming resulted in potassium chloride (*KCl*) salt crystal precipitation on the glauconite grain surfaces. This is a strong indication that the glauconite grains contained water.
3) It was possible to allow water vapour to condensate on the rock surface and observe condensation water drops. Water-drops developed only on quartz and feldspar grains but not on the glauconite. This final test suggests that glauconite grains imbibed the water, not allowing condensation and thereby indicating water-wetness.

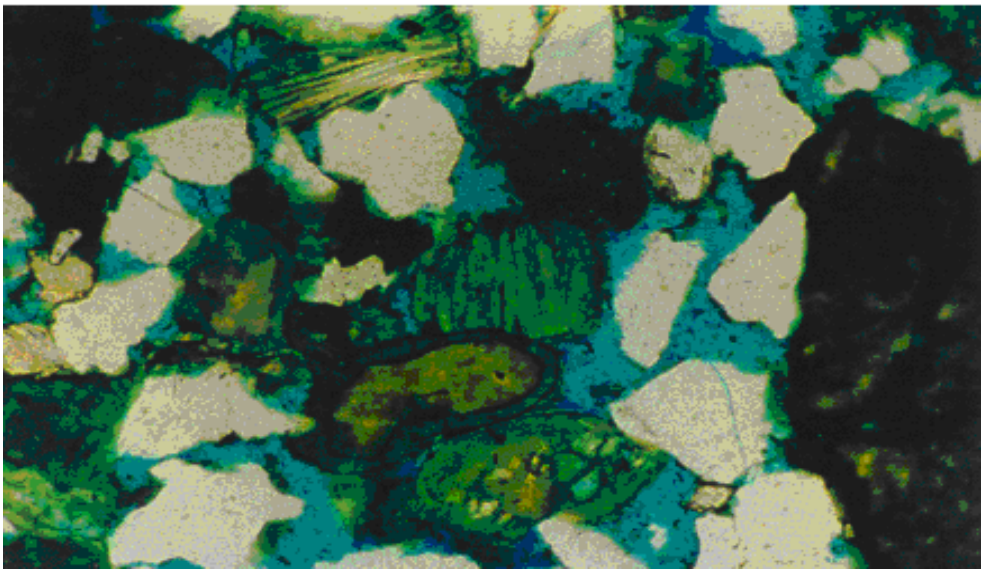

Thin section 2: Illustration of the pellet form of glauconite within the grain framework: three green grains in the center. Magnification x145

Capillary Pressure & Resistivity Measurements

Mercury injection, porous plate gas/water and oil/water measurements were performed on selected plugs from all three wells including both clean and fresh plugs for the oil/water measurements (Figure 3). The g/w primary drainage curves typically showed very high irreducible water saturations. The scaled mercury capillary pressure curves agreed with the gas/water curves for parts of the saturation range. It could be expected that the curves from the mercury test would show a threshold at high capillary pressure and reveal a dual porosity type system based on the high glauconite content, but this was not the case as the figure shows.

The entire set of resistivity index (*RI*) versus saturation experiments had a distinct concave upward shape, as can be seen in Figure 4. This is the opposite of the concave downward shape of the familiar 'shale' effect. The *n*-exponent for fresh samples was generally higher than for clean samples, probably due to the wettability difference between fresh and clean plugs. The clean samples were water-wet and were not believed to be representative of the

reservoir wettability. Conversely, the fresh samples could be too oil-wet due to possible alteration during coring and tests performed at ambient conditions. These differences had to be taken into account as an uncertainty in the evaluation.

It was observed that the n-exponents reported by laboratories are often only based on the endpoint values, whilst others report results derived from linear regressions over all of the S_w range. Given the form of the relationship, this variation in practice could potentially lead to misleading results, Figure 5.

The average end-point based n-exponent for 6 plugs from the second well was 3.0. The same 6 plugs using regression analysis gave an n-exponent of 2.7.

When the field was evaluated, conventional wireline water saturation analysis was undertaken with the Waxman-Smits[4] model using relatively extreme n-exponent values derived from best fits to the core resistivity data. This was found to give an acceptable fit to the *DS* derived values (see log-plot from the second well at the end of the paper) although errors were still observed throughout the cored section. Using this method it could be expected that low water saturations will be under-predicted whilst high water saturations will be over-predicted.

Porosity Measurement

A thorough porosity study was not initiated to explore effective versus total porosity, but by chance a difference was noticed between routine porosity and porosity measured during the special core analysis program. This was investigated further and the drying procedure was shown to affect the porosity (Figure 6). Plugs dried in a humidity-controlled oven (60 degree *C* and 40% humidity) had a lower porosity than plugs dried without humidity control. Even leaving the plug on the bench in the laboratory for a while after drying reduced the porosity compared to it being measured at once. All porosity measurements were Boyle's law, helium expansion. The porosity of humidity dried *SCAL* plugs had to be increased by about 1.5 *P.U.* to correct for the effect of drying (Figure 7). This effect was attributed to glauconite.

Discussion

A decision was made to use total porosity instead of effective porosity. To use effective porosity would require a method for its determination using logs with no core data that appeared impossible. Mapping the glauconite field wide based on core or cuttings from all wells might be a possible approach.

The form of the *RI* vs. S_w curves supports the *ESEM*/petrographical observations of a porous, water filled and water-wet glauconite, which is spread as pellets throughout the sandstone matrix. At low S_w's the glauconite is still primarily water filled, but isolated. This leads to elevated sample resistivity values at these saturations. This effect is the opposite of that normally seen as a result of 'connected' conductive clay coatings. If the

concave upward data are real, then using a traditional straight line, best fit to the resistivity data can result in systematic errors.

Recalculating the *n*-exponent measurements to an effective porosity will eliminate the upward concave shape based on the equation:

$$S_{w,new} = \frac{S_w - f_{mp}}{1 - f_{mp}},$$

where f_{mp} is the fraction of non-connected water filled pore volume (glauconite).

Figure 8 shows an example where the effective pore volume has been calculated based on the assumption of 20% and 30% micro porosity. The resistivity vs. saturation plot will appear closer to a straight line. The *n*-exponents (regression) for the total porosity case is 2.9 whilst for the effective pore system it is reduced to ~1,15 and ~2.0 dependent on the assumed amount of glauconite.

For the residual oil saturation after water flooding the experimental values seemed in general very low but with a scatter. When taking into account only the effective pore system the values became quite "normal" and some of the scatter in the data could be reduced. Table 1 show a comparison of S_{orw} and S_{wi} (initial water saturation in the water flooding experiments) between an effective and a total pore system. The variation in S_{wi} and S_{orw} values in the total pore system is an effect of the amount of glauconite porosity. Operating with an effective pore system, the values appear more consistent.

Table 1: Some typical saturation values for a total and effective pore system

Examples	**Total pore system**				**Effective pore system**		
Plugs from:	Porosity	**S_{wi}**	**S_{or}**	Glauconite *P.U.*	Porosity	**S_{or}**	**S_{wi}**
Main field	32	**40**	**12**	10	22	**17**	**13**
East upper zone	31	**50**	**9**	13	18	**16**	**14**
East lower zone	31	**63**	**7**	18	13	**17**	**12**

It proved to be challenging to communicate the total pore concept in a system heavily affected by micro-'ineffective' porosity within the multi-disciplinary subsurface team and partner group.

By choosing the Waxman-Smits method we introduced a degree of both random and systematic errors that was acceptable in the initial core well dataset. The work conducted here shed more light on the source to systematic errors and therefore allowed a more consistent approach to future well analysis where glauconite volumes may vary significantly.

Conclusions

High content of glauconite grains with high microporosity can be a challenge to special core analyses, and interpretation and implementation of data:

- Standard resistivity log interpretation can indicate low water saturation (high resistivity), while core extraction and capillary drainage indicates high water saturation
- The ESEM technique was used to show that the glauconite inter-grain porosity was water wet and water saturated
- Traditional resistivity index interpretation will not fit the data due to the high content of isolated, water filled grains
- The glauconite resistivity effect is the opposite of the Waxman-Smit type corrections for clay conductivity
- Although using the effective porosity concept would have made SCAL-data interpretation simpler, total porosity had to be used on well and field scale due to lack of glauconite fraction indicators.

This field exploration exercise proved the importance of taking core and determining water saturation directly on the cores. The effect of the glauconite shows that unusual results make detailed mineralogical description and interpretation necessary.

Acknowledgement

Tony Boassen who conducted the ESEM experiment.

References

[1] "Recommended Practices for Core Analysis", American Petroleum Institute, API40 (Feb. 1998)
[2] Ringen J.K., Halvorsen, C., Lehne, K.A., Hoeland, H. "Reservoir water saturation from cores and its use in log evaluation", paper SCA-9906, (1999)
[3] Robin, M, Combes, R., Degreve, F., Cuiec, L. "Wettability of porous media from ESEM; from model to reservoir rocks", paper SPE 37235, (1997)
[4] Waxman, M.H. & Smits, L.J.M. 'Electrical Conductivities in Oil-Bearing Shaly Sands' *Society of Petroleum Engineers Journal*, (June 1968), 107-119. *Trans.*, AIME **243**

Nomenclature

C	Celsius
DS	Dean - Stark
$ESEM$	Environmental Scanning Electron Microscope
f_{mp}	Fraction of micro pores
n, n-exponent	Archie saturation exponent

$P.U.$	Porosity Units
RI	Resistivity Index
S_{orw}	Residual oil saturation after water flooding
S_w	Water saturation
S_{wi}	Water saturation, initial

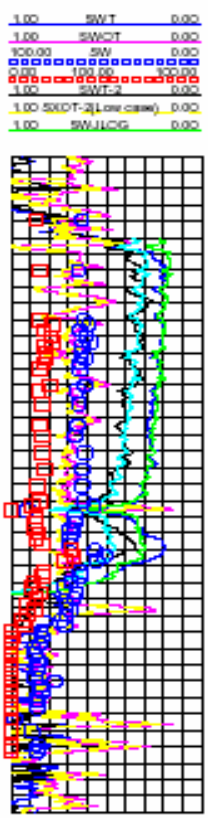

Figure 1: Discovery well

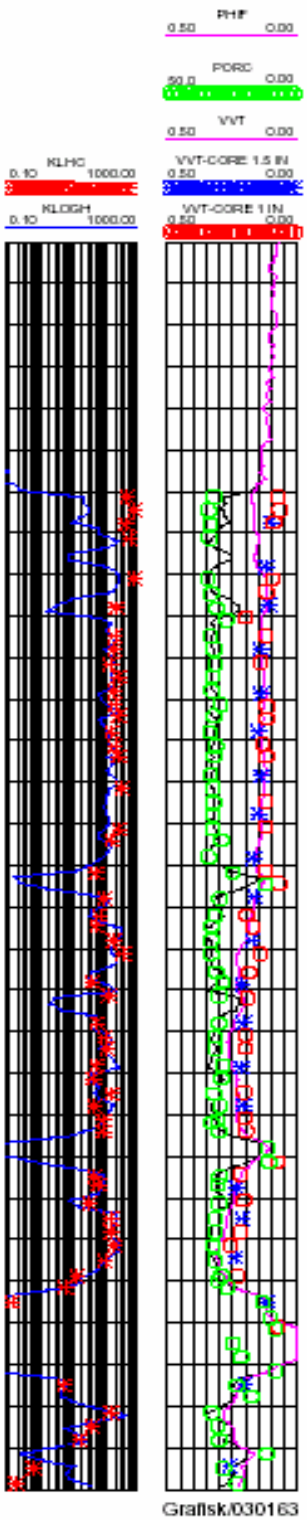

Figure 2: Second well

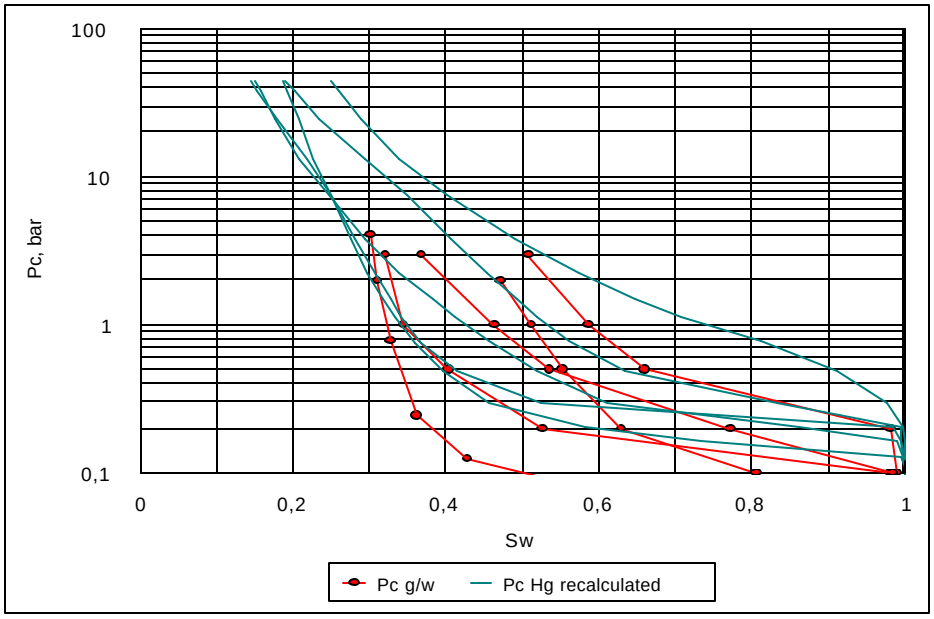

Figure 3: g/w capillary pressure drainage curves from porous plate and mercury injection recalculated to g/w.

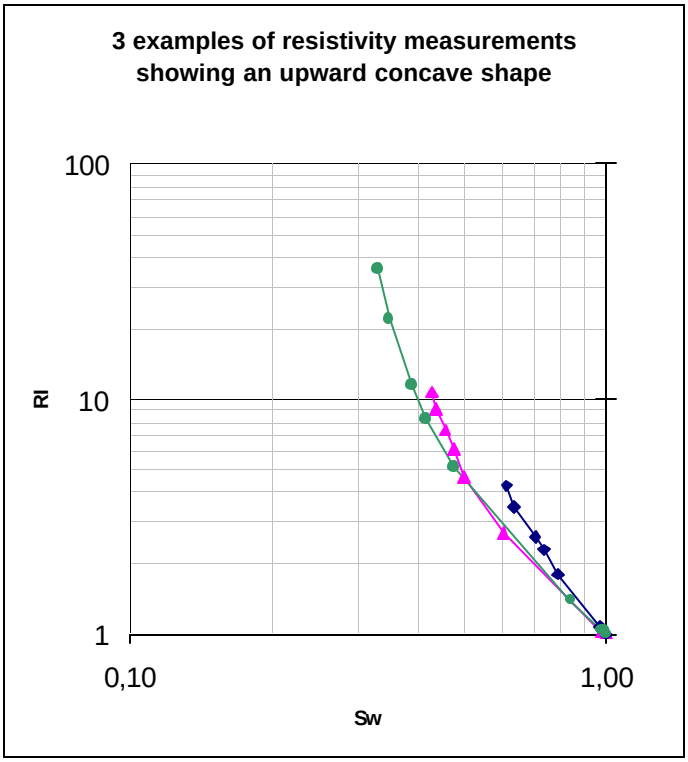

Figure 4: Resistivity index measurements

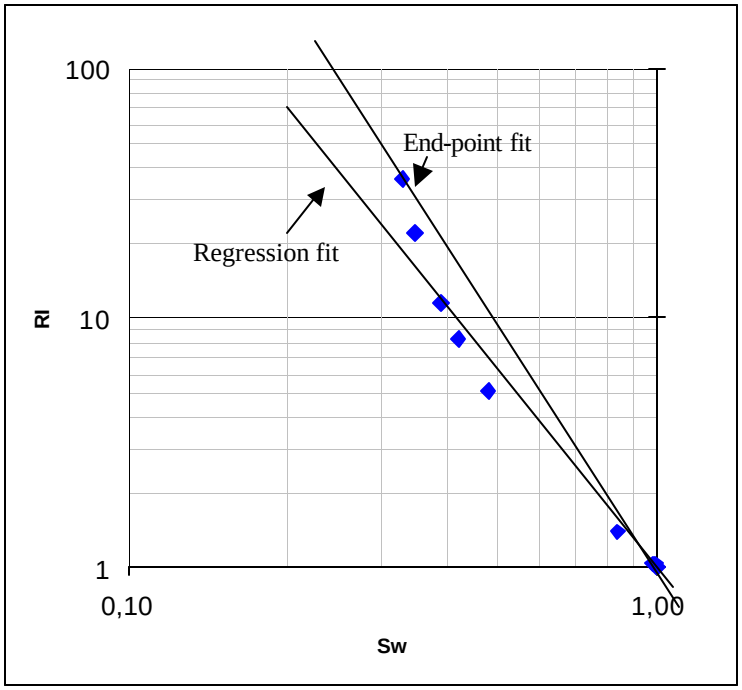

Figure 5: Example of different interpretation of the measured *RI* vs. S_w data

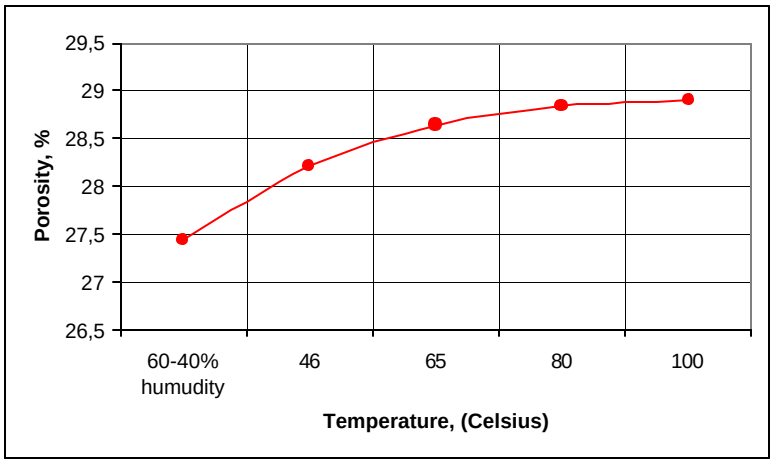

Figure 6: Plot of porosity vs. drying temperature & humidity, average of 4 samples.

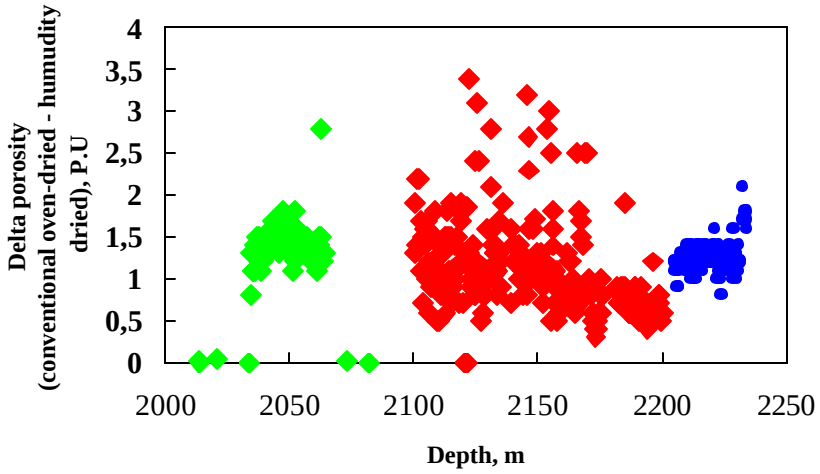

Figure 7: Plot of difference in porosity determined after conventional drying and humidity drying vs. depth for three wells (three colours)

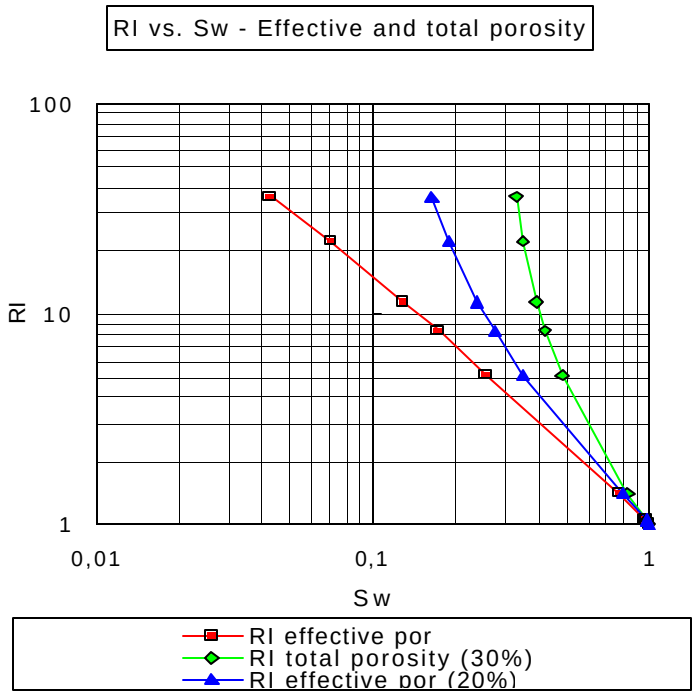

Figure 8: Examples of resistivity measurements and effect of micro porosity